Journal of Process Control 76 (2019) 15–26

Contents lists available at ScienceDirect

Journal of Process Control

journal homepage: www.elsevier.com/locate/jprocont

Accounting for dynamics in self-optimizing control

Jonatan Ralf Axel Klemets*, Morten Hovd

Department of Engineering Cybernetics, Norwegian University of Science and Technology, Trondheim, Norway

ARTICLE INFO

Article history:
Received 13 July 2018
Received in revised form 3 January 2019
Accepted 13 January 2019
Available online 19 February 2019

Keywords:
Self-optimizing control
LMI
Control structure design
Static output feedback control

ABSTRACT

Self-optimizing control focuses on minimizing the steady-state loss for processes in the presence of disturbances by holding selected controlled variables at constant set-points. The loss can further be reduced by controlling linear measurement combinations that have been obtained with the purpose of minimizing either the worst-case loss or the average loss. Since self-optimizing control mainly focuses on the steady-state operation, little emphasis has been put on the dynamic behaviour of the resulting closed-loop system. The general approach is to first compute the optimal controlled variables and then design their respective controllers. However, the optimal measurement combinations, can often (especially if many measurements are used) result in very dynamically complex systems, that makes designing the feedback controllers difficult. In this work, PI controllers and measurement combinations are simultaneously obtained with the aim to find an optimal trade-off between minimizing the steady-state loss and the transient response for the resulting closed-loop system. A solution can be found by solving a bilinear matrix inequality (BMI), which becomes a linear matrix inequality (LMI) by specifying a stabilizing state feedback gain. The optimization problem can also be combined with the sparsity promoting weighted l_1-norm, which penalizes the number measurements used and thus, attempts to find an optimal measurement subset. The proposed method requires solving a BMI, for which an iterative LMI approach can be used to find a local optimum, which often seems to give good results, as illustrated on two case studies, consisting of a binary and a Kaibel distillation column.

1. Introduction

The ever-increasing competitive pressure in the global markets results in the need for continuously improving the performance of chemical processes. Operating the process close to its economically optimal operating point is thus essential. This leads to higher demands on the control system, which has to ensure that the plant is kept close to the desired operating point. If there are large deviations from the optimal operation, caused by, e.g., external disturbances, it would evidently result in an economic loss and could violate some of the operating constraints. Therefore, both the steady-state (economic) objective and the dynamic performance of the process should be considered when designing the control system.

Chemical process plants are typically operated with the aid of a multilayer hierarchical control structure, consisting of several layers that address different time scales [1,2]. Traditionally, the economic optimization and the dynamic control of chemical processes are separated and operate at different layers. The economic optimization is usually located in an upper layer and uses real-time optimization (RTO) [3] to compute and send the optimal set-points to the lower layers. The role of the lower layer is to drive the process to the desired set-point using, e.g., model predictive control (MPC) or other low-level controllers (typically PID Controllers). Recently there has been an increasing interest in economic model predictive control (EMPC) [4], which attempts to integrate the economic optimization and process control performance together. Despite the recent advancements, there are still challenges when it comes to implementation in real processes, mainly due to the computational complexity and requirement for accurate dynamic models of the process.

Another approach is to use simple control structures that keep specific controlled variables at a constant value, also known as self-optimizing control [5]. The central idea of self-optimizing control is to select controlled variables such that in the presence of disturbances, the loss is minimized by holding the chosen controlled variables at constant set-points. Beyond using single measurements, selecting linear combinations of measurements as controlled variables will further improve the self-optimizing control performance. Two methods that achieve this are the exact local

* Corresponding author.
E-mail addresses: jonatan.klemets@ntnu.no (J.R.A. Klemets), morten.hovd@ntnu.no (M. Hovd).

https://doi.org/10.1016/j.jprocont.2019.01.003

method [6] and the null-space method [7]. Most research on self-optimizing control (see, e.g., the survey paper by [8]) is mainly concerned with the steady-state operation without considering the dynamic behaviour of the resulting closed-loop system. This can lead to dynamically complex systems with e.g., right hand-plane zeros at low frequencies that poses limitations on the achievable control performance. Therefore, it would be preferable to find a combination that also takes the dynamic behaviour into account. However, the resulting closed-loop system is not just dependent on the measurement combination, but also on the feedback controllers.

The proportional integral (PI) controller is by far the most commonly used controller in the process industries due to its simplicity and robust performance [9]. With progress in numerical methods, new convex optimization methods have been developed for designing controllers. However, for restricted-order controllers (e.g., PI/PID controller) the optimization problems tend to become non-convex in the controller parameter space. They are usually solved by employing heuristics or intelligent methods [10,11]. A loop shaping method was proposed in [12], by specifying bounds on the phase and gain margins.

These methods often aim to minimize some common control performance criterion, e.g., the integrated absolute error (IAE). However, in self-optimizing control (SOC) minimizing IAE may not be ideal. Typically, the SOC variables are controlled by the remaining degrees of freedom, once the plant first has been stabilized and all the active constraints are being controlled. Although it is economically optimal to operate the plant as close as possible to its active constraints, it is usually necessary to employ some "back off" to avoid dynamic and steady-state problems. "Back off" is the difference between the optimal set-point and the actual set-point, and is estimated based on the information of the disturbances and the expected control performance [13,14]. Therefore, the SOC variables should preferably, when subjected to disturbances, drive the process to the new optimal operating point while minimizing deviations in the active constraints (i.e., reducing the "back off") or in other variables with large economic impact.

Instead, of minimizing IAE, it might be better to find the SOC variables by recasting it as an optimization problem for finding, e.g., the H_2 or the H_∞ optimal static output feedback (SOF) controller that minimizes the deviations in a specified performance output. Contrary to full state-feedback or full-order controllers, which can be solved using Linear Matrix Inequalities (LMI), structured static output feedback generally results in Bilinear Matrix Inequalities (BMI) and remains an open problem [15,16]. They are often solved to a local optimum by iteratively fixing some variables and solving the resulting LMI.

The optimal measurement combination has been shown to be non-unique, and if multiplied with any non-singular matrix it results in the same steady-state loss. Based on [17,18], an iterative LMI algorithm was proposed in [19] for simultaneously determining this non-singular matrix and PI controller parameters to improve the dynamic performance. However, the optimal self-optimizing control variable is only non-unique if the degrees of freedom available are greater than one. Furthermore, while [19] maintains the optimal steady-state solution, it may be beneficial to choose a measurement combination with a larger steady-state loss if it would provide a significant improvement in the closed-loop performance. That is, if the dynamic improvements resulted in better disturbance rejection, it could allow for a reduction in the "back off" applied to the active constraints and as a consequence further increase the profitability.

Therefore, in this work, an iterative LMI algorithm is proposed that solves a Pareto optimization problem that gives a trade-off between minimizing the steady-state loss and the dynamic performance. The proposed method can then be expanded on as in [20], to include an additional penalty function in the multi-objective optimization problem that promotes sparsity by penalizing the number of measurements used. The sparsity promoting function is known as the weighted l_1-norm [21], and has been used in several papers for promoting sparsity in controller design, see, e.g., [22–24]. The proposed method is validated by applications to models of a binary and a Kaibel distillation column.

The paper is organized as follows. Section 2 introduces the notation used in this paper while the concept of self-optimizing control is described in Section 3. The main contribution is presented in Section 4, where the optimization problem of finding a measurement combination together with PI controllers is formulated as a BMI. The optimization problem is solved to a local optimum using an iterative LMI algorithm. In Section 5, results from simulations are presented, where the proposed method has been used to design the control structures for two different distillation column models. Finally, a conclusion is given in Section 6.

2. Preliminaries

Let $\mathbb{R}^{n\times m}$ denote the set of $n \times m$ real matrices. For a matrix A, its transpose is denoted A^T, and A^{-1} denotes its inverse. The identity and the null matrix of suitable dimension is given by I and 0. The notation $A \prec 0, A \succ 0$ means the matrix is positive and negative definite respectively. $\|\cdot\|_1$, $\|\cdot\|_2$,$\|\cdot\|_\infty$, and $\|\cdot\|_F$ represents the l_1, H_2, H_∞, and Frobenius norms, respectively.

3. Self-optimizing control

Self-optimizing control is achieved when an acceptable loss is obtained with constant set-points without the need to reoptimize when (changes in) disturbances occur [5]. More precisely, the aim is to select controlled variables rather than determining optimal set-points. Here, the loss L is defined as the difference between the actual value of a given cost function and the truly optimal value (accounting for the correct value of the disturbance), i.e.,

$$L(u, d) = J(u, d) - J_{opt}(d), \tag{1}$$

where truly optimal operation is achieved when $L = 0$. However, in general, $L \geq 0$ and thus a smaller value for the loss function, L implies that the plant is operating closer to its optimum. By using the available degrees of freedom (u), the goal is to minimize the constrained cost function (J), in order to find the optimal operating point for the process. Typically, J defines the economic cost of the process and can often be expressed as

$$J = \text{feed cost} + \text{utilities cost} - \text{product value}.$$

However, other objectives such as energy efficiency and indirect control [25] are also possible.

For specified disturbances (d), the optimization problem can be formulated as,

$$\min_{x,u} \quad J(x, u, d) \tag{2}$$

$$\text{s.t.}\, f(x, u, d) = 0 \tag{3}$$

$$g(x, u, d) \leq 0 \tag{4}$$

$$y = f_y(x, u, d) \tag{5}$$

where $x \in \mathbb{R}^{n_x}$, $u \in \mathbb{R}^{n_u}$, and $d \in \mathbb{R}^{n_d}$ are the states, inputs, and disturbances respectively. The equality constraints are represented by $f(\cdot)$ and contain the steady-state model equations; the inequality constraints in $g(\cdot)$ define the constraints on the operation, and the available measurements are given by y. The solution to the

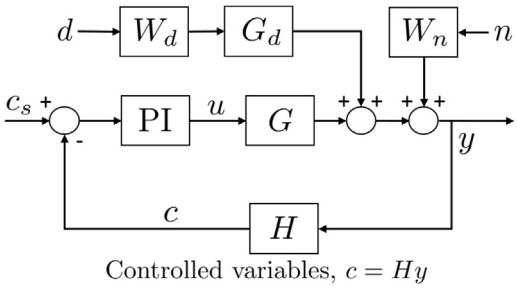

Fig. 1. Block diagram of the self-optimizing control structure.

optimization problem usually results in some of the constraints being active, i.e., $g_i(x, u, d) = 0$. To achieve optimal operation at steady-state, the variables related to the active constraints should be controlled and kept as close as possible to their optimal set-points. Stabilizing the plant and controlling the active constraints, therefore, requires a corresponding number of degrees of freedom. Under the assumption that the active constraints remain the same during operation, then it results in the reduced space optimization problem:

$$\min_u J^*(u, d). \tag{6}$$

Here, the model equations and active constraints, are implicitly included in J^*. What remains is to determine which of unconstrained controlled variables (y and u) that should be kept at constant set-point by using the remaining degrees of freedom (u), in order to minimize loss. To quantify the loss resulting from keeping the selected controlled variables at constant values, methods for calculating the worst case and average loss were derived in [6,26] respectively.

3.1. Optimal measurement combination

Rather than selecting single measurements for the unconstrained optimization problem in (6), a further reduction in loss can be obtained by selecting the control variables as optimal linear measurement combinations $c = Hy$, resulting in the control structure seen in Fig. 1. The matrix $H \in \mathbb{R}^{n_u \times n_y}$ defines the measurement combinations, and $y \in \mathbb{R}^{n_y}$ is a subset of the available measurements.

3.1.1. The exact local method

With the expectation operator denoted $\mathbb{E}[\cdot]$, and assuming the disturbances d and measurement noise n are independent and uniformly distributed in the sets $d \in \mathcal{D}$, and $n \in \mathcal{N}$. Then, the worst case and average loss were derived in [6,26] respectively and are given by

$$L_{worst} = \max_{d\in\mathcal{D}, n\in\mathcal{N}} L = \frac{1}{2}\|J_{uu}^{1/2}(HG^y)^{-1}HY\|_2^2, \tag{7}$$

$$L_{avg} = \mathop{\mathbb{E}}_{d\in\mathcal{D}, n\in\mathcal{N}}[L] = \frac{1}{2}\|J_{uu}^{1/2}(HG^y)^{-1}HY\|_F^2. \tag{8}$$

Here, $Y := \begin{bmatrix} FW_d & W_n \end{bmatrix}$, with W_d and W_n representing the expected magnitudes of the disturbances and implementation errors respectively. $F = \frac{\partial y^{opt}}{\partial d}$ is the sensitivity matrix for the optimal deviations in the measurements (∂y^{opt}) with respect to changes in the disturbances (∂d); $J_{uu} = \frac{\partial^2 J}{\partial u^2}$ denotes the second derivative of the cost function (6), and $G^y = \frac{\partial y}{\partial u}$, represents the gain from the inputs to the available measurements. The authors of [26] proved that obtaining the H that minimizes the average loss in (8) is super-optimal and hence, the same H also minimizes the worst case loss in (7). However, the opposite is not necessarily true. Therefore, only the minimization of the Frobenius norm will be considered in this paper, where the optimization problem can be formulated as

$$\min_H \frac{1}{2}\|J_{uu}^{1/2}(HG^y)^{-1}HY\|_F^2. \tag{9}$$

At first glance, this seems like a non-linear optimization problem. However, an important observation was discovered in [27], which found that (9) can be recast as a convex optimization problem.

Theorem 1. *If H is a full matrix (with no structural constraints) then the problem in (9) can be formulated as a convex constrained optimization problem [27]:*

$$\min_H \frac{1}{2}\|HY\|_F^2 \tag{10}$$

$$\text{s.t. } HG^y = J_{uu}^{1/2} \tag{11}$$

Proof. From the original problem in (9), it can be shown that the optimal solution for H is non-unique and for any non-singular matrix $Q \in \mathbb{R}^{n_u \times n_u}$,

$$\hat{H} = Q^{-1}H \tag{12}$$

results in the same loss. This can be shown by [8]:

$$\begin{aligned} L_{avg} &= \frac{1}{2}\|J_{uu}^{1/2}(\hat{H}G^y)^{-1}\hat{H}Y\|_F^2 \\ &= \frac{1}{2}\|J_{uu}^{1/2}(Q^{-1}HG^y)^{-1}Q^{-1}HY\|_F^2 \\ &= \frac{1}{2}\|J_{uu}^{1/2}(HG^y)^{-1}QQ^{-1}HY\|_F^2 \\ &= \frac{1}{2}\|J_{uu}^{1/2}(HG^y)^{-1}HY\|_F^2. \end{aligned} \tag{13}$$

The non-uniqueness of H can be used to add the constraint in (11), which guarantees that the first part in (9) becomes $J_{uu}^{1/2}(HG^y)^{-1} = I$. Hence, the nonlinear optimization in (9) can be recast as the convex optimization problem in (10) and (11).

Remark 1. Some additional insight was given in [28], where it was noted that J_{uu} is not needed for finding the optimal H in (10) and (11).

This means J_{uu} can be replaced with any non-singular matrix Q and still give the optimal H. This may simplify the calculations, as J_{uu} can be difficult to obtain numerically. However, J_{uu} would still be required to find the correct numerical value of the loss.

Remark 2. For a measurement combination H with $n_u \geq 2$, a non-singular matrix Q can be chosen as in (12), to get a measurement combination with better dynamic properties while still maintaining the same steady-state loss.

The optimal solution to (10) provides the measurement combination that gives the locally best steady-state performance. However, the optimal solution does not consider the resulting transient response and can give rise to complex dynamic behaviour. If $n_u \geq 2$, then a non-singular matrix Q can be selected to get a measurement combination with better dynamic behaviour without affecting steady-state performance. However, if $n_u = 1$, then Q becomes a scalar and can only change the steady-state gain of $\hat{H}$ with no effect on the dynamic behaviour. Furthermore, even if $n_u \geq 2$ it may be beneficial to sacrifice some steady-state loss if it

significantly improves the closed-loop performance. Therefore, a method is proposed in Section 4 that tries to obtain the optimal trade-off between the steady-state and dynamic performance.

3.2. Selecting a measurement subset

The lowest steady-state loss can be achieved when the measurement combination H is computed using all available measurements. However, for most practical cases this is not desirable as it leads to overly complex control structures and increases the likelihood of getting sensor failures. Besides, often, there exists a subset of the available measurements that can be used without any significant reduction in the steady-state performance.

Finding the best measurement subset is a combinatorial optimization problem, and the loss has to be evaluated at every possible measurement combination. To solve this problem, [29] developed a tailor-made branch and bound algorithm. Another approach was presented in [28], where the combinatorial problem was formulated using mixed integer quadratic programming (MIQP) that can be solved using standard MIQP solvers.

An alternative approach, for finding the optimal measurement subset is to solve a multi-objective optimization problem, that gives the optimal trade-off between steady-state loss and the number of measurements used. If a column-wise sparsity promoting function is included in (10), the optimization problem can be formulated as,

$$J = \min_{H} \frac{1}{2}\|HY\|_F^2 + \lambda \; card(H) \tag{14}$$

subject to (11). By specifying a scalar value for λ, there will be a trade-off between the steady-state loss and the cardinality of H, where the cardinality of the measurement matrix H is defined:

$$card(H) := \textit{the number of } \text{non} - \text{zero } \textit{columns of } H.$$

The cardinality function is non-convex and non-smooth, that still makes the optimization formulation in (14) a combinatorial problem, which is difficult to solve.

To address this issue, several convex relaxations like the l_1-norm and the weighted l_1-norm have been proposed [21]. By using the weighted l_1-norm, the cardinality function can be replaced with:

$$card(H) = \sum_{i,j} W_{i,j}\|H_{i,j}\|_1 \tag{15}$$

The authors of [21] noted that if the weights $W_{i,j}$ are chosen to be inversely proportional to the l_1-norm, then there is an exact correspondence between the l_1-norm and the cardinality function. However, this requires *a priori* knowledge of the H matrix, and therefore, a re-weighted scheme needs to be implemented, where the weights are updated after every iteration (k) as,

$$W_{i,j}^{(k+1)} = \frac{1}{\|H_{i,j}^{(k)}\|_1 + \kappa} \tag{16}$$

where $1 \gg \kappa > 0$ ensures the update is well-defined.

The weighted l_1-norm in (15) promotes element-wise sparsity. However, it can easily be modified to promote column (or row) sparsity as, e.g., shown in [30] by revising it as,

$$card(H) = \sum_{i,j} W_j\|H_{i,j}\|_1 \tag{17}$$

with the update rule:

$$W_j^{(k+1)} = \frac{1}{\sum_i \|H_{i,j}^{(k)}\|_1 + \kappa} \tag{18}$$

For a given value of λ, the iterative procedure, described in Algorithm 1 can be used to find a subset of the available measurements.

Algorithm 1:

Initialize: obtain H, by solving (10) s.t. (11) and compute $W^{(k)}$ using (18).

1: For the obtained $W^{(k)}$ solve:
$$J_k = \min_{H} \frac{1}{2}\|HY\|_F^2 + \lambda \sum_{i,j} W_j^{(k)}\|H_{i,j}\|_1$$
s.t. (11).

2: If $\|H^{(k-1)} - H^{(k)}\|_2 < \epsilon$ go to step 3, else update $W^{(k+1)}$ using (18) and repeat step 1 and 2.

3: Remove the measurements that correspond to the zero columns in H.

While the convergence properties for the re-weighted l_1-norm are still not clearly understood, numerical experiments have shown it to be a very efficient method for promoting sparsity, which also is demonstrated in Section 5.1.1.

4. Static output feedback control

In self-optimizing control, the focus mainly lies on the economic steady-state behaviour. However, in the resulting closed-loop system shown in Fig. 1, it can be seen that the dynamic behaviour is heavily dependent on both the measurement combination H and the PI controller. Thus, when determining H, it would be advantageous to consider both the steady-state and the dynamic behaviour of the resulting closed-loop system.

In this section, the method for simultaneously selecting the measurement combination and designing the feedback controllers is presented. The method is based on the two-step procedure for static output feedback controller design, which is similar to [17,18,31–33]. These methods formulate the optimization problem as a bilinear matrix inequality (BMI) that becomes linear matrix inequalities (LMI), if initialized with a stabilizing state feedback controller.

4.1. Process model and PI controllers

Consider a system described by the discrete linear time-invariant state-space model,

$$x_{k+1} = A_x x_k + B_u u_k + B_w w_k \tag{19}$$

$$y_k = C_{yx} x_k + D_{yw} w_k \tag{20}$$

where $x_k \in \mathbb{R}^{n_x}$, $y_k \in \mathbb{R}^{n_y}$, $u_k \in \mathbb{R}^{n_u}$, $w_k \in \mathbb{R}^{n_w}$ are the states, measurements, inputs, and disturbances respectively. The aim is to find a measurement combination matrix $\hat{H}$ and design a feedback controller that gives the desired trade-off between the steady-state and dynamic performance. Due to their popularity in the industry, decentralized PI controllers will be used as the feedback controllers. In their ideal form, they are represented by

$$u_k = K_p(e_k + K_i \sum_{n=0}^{k-1} e_n), \tag{21}$$

where $u_k \in \mathbb{R}^{n_u}$ and $e_k \in \mathbb{R}^{n_u}$ represent the control variable and the error value of the PI controller. The parameters $K_p \in \mathbb{R}^{n_u \times n_u}$ and $K_i \in \mathbb{R}^{n_u \times n_u}$ are diagonal matrices, representing the proportional and integral gains respectively. Here, the sampling time is assumed to be included in K_i, i.e., K_i varies depending on the sampling time. When a measurement combination $\hat{H}$ is used, then the error value is defined $e_k := r_k - \hat{H}y_k$, where r_k is the reference input. Setting the reference value to $r_k = 0$ (using deviation variables), the error value becomes $e_k = -\hat{H}y_k$, and thus, the PI controller in (21) can be expressed as:

$$u_k = -K_p(\hat{H}y_k + K_i \sum_{n=0}^{k-1} \hat{H}y_n) \tag{22}$$

From the above formulation, it can be seen that this description is overparameterized, where K_p can be considered as a simple scaling value for $\hat{H}$. Therefore, K_p can be selected to be any non-zero value, e.g., setting $K_p = I$ gives:

$$u_k = -(\hat{H}y_k + K_i\sum_{n=0}^{k-1}\hat{H}y_n) \tag{23}$$

Defining an auxiliary state vector $q_k \in \mathbb{R}^{n_u}$ for the integral term (the summation term $\sum_{n=0}^{k-1}\hat{H}y_n$), then the state space representation of the PI controller in (23) becomes:

$$\begin{bmatrix} u_k \\ q_k \end{bmatrix} = \begin{bmatrix} -(\hat{H}y_k + K_i q_{k-1}) \\ q_{k-1} + \hat{H}y_k \end{bmatrix}. \tag{24}$$

By introducing the augmented state vector $\bar{x}_k \in \mathbb{R}^{(n_x+n_u)}$

$$\bar{x}_k := \begin{bmatrix} x_k \\ q_{k-1} \end{bmatrix}, \tag{25}$$

the augmented measurement vector $\bar{y}_k \in \mathbb{R}^{(n_y+n_u)}$

$$\bar{y}_k := \begin{bmatrix} y_k \\ q_{k-1} \end{bmatrix}, \tag{26}$$

and the augmented control input vector $\bar{u}_k \in \mathbb{R}^{2n_u}$, given by the control law:

$$\bar{u}_k := -\begin{bmatrix} \hat{H}y_k \\ K_i q_{k-1} \end{bmatrix}. \tag{27}$$

Then the closed loop system for the process model in (19) and (20) with the PI controllers in (24) can be given by the augmented model

$$\bar{x}_{k+1} = \bar{A}_x\bar{x}_k + \bar{B}_u\bar{u}_k + \bar{B}_w w_k \tag{28}$$

$$\bar{y}_k = \bar{C}_{yx}\bar{x}_k + \bar{D}_{yw}w_k \tag{29}$$

where the augmented system matrices are:

$$\begin{aligned} \bar{A}_x &= \begin{bmatrix} A_x & 0 \\ 0 & I \end{bmatrix}, \quad \bar{B}_u = \begin{bmatrix} B_u & B_u \\ I & 0 \end{bmatrix}, \quad \bar{B}_w = \begin{bmatrix} B_w \\ 0 \end{bmatrix}, \\ \bar{C}_{yx} &= \begin{bmatrix} C_{yx} & 0 \\ 0 & I \end{bmatrix}, \quad \bar{D}_{yw} = \begin{bmatrix} D_{yw} \\ 0 \end{bmatrix}. \end{aligned} \tag{30}$$

Using the proposed control law for $\bar{u}_k$ in (27), which is equivalent to

$$\bar{u}_k = -\begin{bmatrix} \hat{H} & 0 \\ 0 & K_i \end{bmatrix}\bar{C}_{yx}\bar{x}_k - \begin{bmatrix} \hat{H} & 0 \\ 0 & K_i \end{bmatrix}\bar{D}_{yw}w_k, \tag{31}$$

$$= -\begin{bmatrix} \hat{H}C_{yx}x_k + \hat{H}D_{yw}w_k \\ K_i q_{k-1} \end{bmatrix}. \tag{32}$$

Then it can easily be shown that the augmented process model in (28) and (29) becomes

$$\begin{bmatrix} x_{k+1} \\ q_k \end{bmatrix} = \begin{bmatrix} A_x x_k - B_u(\hat{H}y_k + K_i q_{k-1}) + B_w w_k \\ q_{k-1} + \hat{H}y_k \end{bmatrix},$$

which corresponds to a closed-loop system for (19) and (20) with the PI controllers in (24).

The proposed augmented system in (28) and (29) differs from how state space models typically are augmented with PI controllers [34,35]. E.g., in (27) the length of the augmented control input vector $\bar{u}_k$ have been doubled by separating $\hat{H}y_k$, and $K_i\sum_{n=0}^{k-1}\hat{H}y_n$ from each other in (23). The benefit of this approach is that $\hat{H}$ and K_i are decoupled in the control law (31), which will be beneficial when computing their values in Section 4.2.

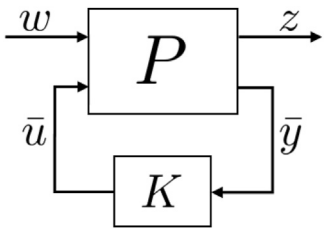

Fig. 2. Control configuration for static output feedback control.

It is possible that better performance can be achieved if more advanced controller formulations are used instead of decentralized PI controllers. The main difference would be how the controller description is included in the formulation of the augmented system matrices in (30). One important requirement is that the controllers incorporate some integral action to ensure that the self-optimizing control criterion is met at steady-state. However, the simulations in Section 5.2, and the work in [20] seems to indicate that well-tuned decentralized PI controllers can give comparable results to more advanced control structures if the controlled variables (measurement combinations) are chosen properly. Also, using a decentralized PI control structure allows for relatively easy retuning of the controllers, when comparing to the case using advanced multivariable controllers, should future changes in operating conditions make retuning necessary. Thus, the small potential improvements in performance for more advanced control strategies may not be worth their additional complexity.

4.2. H_∞ static output feedback control

Consider the following generalized extension of the augmented system in (28) and (29):

$$P: \begin{cases} \bar{x}_{k+1} &= \bar{A}_x\bar{x}_k + \bar{B}_u\bar{u}_k + \bar{B}_w w_k \\ \bar{y}_k &= \bar{C}_{yx}\bar{x}_k + \bar{D}_{yw}w_k \\ z_k &= \bar{C}_{zx}\bar{x}_k + \bar{D}_{zu}\bar{u}_k + \bar{D}_{zw}w_k \end{cases} \tag{33}$$

where $z_k \in \mathbb{R}^{n_z}$ is the performance output vector. The augmented plant P maps the exogenous disturbance inputs w_k and the control inputs $\bar{u}_k$ to the performance output z_k and the measured outputs $\bar{y}_k$ as shown in Fig. 2.

The H_∞ optimal control problem then consists of minimizing the H_∞-norm of the closed-loop system from the exogenous disturbance signals w_k to the performance output signals z_k [36,37]. Defining the closed loop matrices,

$$A_{cl} = \bar{A}_x + \bar{B}_u K\bar{C}_{yx} \tag{34}$$

$$B_{cl} = \bar{B}_d + \bar{B}_u K\bar{D}_{yw} \tag{35}$$

$$C_{cl} = \bar{C}_{zx} + \bar{D}_{zu}K\bar{C}_{yx} \tag{36}$$

$$D_{cl} = \bar{D}_{zw} + \bar{D}_{zu}K\bar{D}_{yw} \tag{37}$$

where K is the static output feedback controller. When a state feedback controller is used, then $K\bar{C}_{yx}$, $K\bar{D}_{yw}$, $K\bar{C}_{yx}$, and $K\bar{D}_{yw}$ in (34)–(37) are replaced with the state feedback gain K_{SF}. If the resulting closed-loop system is defined as

$$T_{w,z} := \left[\begin{array}{c|c} A_{cl} & B_{cl} \\ \hline C_{cl} & D_{cl} \end{array}\right], \tag{38}$$

then the objective is to find the static output feedback controller K such that $\|T_{w,z}\|_\infty$ is minimized. The H_∞-norm has several interpre-

tations regarding performance. One is that it minimizes the peak of the singular value of $T_{w,z}(j\omega)$. Alternatively, from a time domain interpretation, it can be considered as the worst-case 2-norm [37]:

$$\|T_{w,z}\|_\infty = \max_{w(t)\neq 0} \frac{\|z(t)\|_2}{\|w(t)\|_2}. \tag{39}$$

Next, lets recall the well-known Bounded Real Lemma.

Lemma 1. *(Bounded Real Lemma [36]), $T_{w,z}$ is asymptotically stable and $\|T_{w,z}\|_\infty < \gamma$ iff there exists a symmetric matrix $P \succ 0$ such that the following inequality holds:*

$$\begin{bmatrix} A_{cl}^T P A_{cl} - P & A_{cl}^T P B_{cl} & C_{cl}^T \\ B_{cl}^T P A_{cl} & B_{cl}^T P B_{cl} - \gamma^2 I & D_{cl}^T \\ C_{cl} & D_{cl} & -I \end{bmatrix} \prec 0 \tag{40}$$

Lemma 2. Projection Lemma [38]

Given a symmetric matrix Ψ and two matrices U and V, there exists a matrix Ξ that satisfies

$$U^T \Xi V + V^T \Xi U + \Psi \prec 0 \tag{41}$$

iff the following projection inequalities are satisfied:

$$N_U^T \Psi N_U \prec 0 \tag{42}$$

$$N_V^T \Psi N_V \prec 0 \tag{43}$$

*where N_U and N_V are arbitrary matrices whose columns form a basis of the null spaces of U and V, respectively.*Based on *Lemmas 1 and 2*, an H_∞ optimal solution for $\hat{H}$, and K_i that ensures a stable closed-loop and a minimum upper bound γ for $\|T_{w,z}\|_\infty$ can be obtained from the following theorem.

Theorem 2. *There exist decentralized PI controllers and a measurement combination $\hat{H} \in \mathbb{R}^{n_u \times n_y}$, that gives a stable closed-loop system and minimizes γ while achieving $\|T_{w,z}\|_\infty \leq \gamma$, if there exists a stabilizing state feedback gain $K_{SF} \in \mathbb{R}^{2n_u \times (n_x+n_u)}$, a matrix $H \in \mathbb{R}^{n_u \times n_y}$, a non-singular matrix $Q \in \mathbb{R}^{(n_u \times n_u)}$, a matrix $P = P^T \in \mathbb{R}^{(n_x+n_u)\times(n_x+n_u)}$, diagonalmatrices $X_1, X_2 \in \mathbb{R}^{2n_u \times 2n_u}$, where X_1 has to be invertible, and matrices $Z_1, Z_2 \in \mathbb{R}^{(n_x+n_u)\times(n_x+n_u)}$ that solves the following non-convex optimization problem:*

$$J_k = \min_{K_{SF}, Z_1, Z_2, P, X_1, X_2, Q, H} \gamma^2 \tag{44}$$

$$\text{s.t. } P \succ 0 \tag{45}$$

$$M + N \prec 0 \tag{46}$$

$$X_1 = diag(x_{1_1} \cdots x_{1_{n_u}}) \tag{47}$$

$$X_2 = diag(x_{2_1} \cdots x_{2_{n_u}}) \tag{48}$$

where M is defined

$$M := \begin{bmatrix} \Theta_{11} & * & * & * & * \\ \Theta_{21} & \Theta_{22} & * & * & * \\ \bar{B}_u^T Z_2^T & \bar{B}_u^T Z_1^T & 0 & * & * \\ \Theta_{41} & 0 & \bar{D}_{zu} & -I & * \\ \bar{B}_w^T Z_2^T & \bar{B}_w^T Z_1^T & 0 & \bar{D}_{zw}^T & -\gamma^2 I \end{bmatrix} \tag{49}$$

with

$$\begin{aligned} \Theta_{11} &= -P + (\bar{A}_x + \bar{B}_u K_{SF})^T Z_2^T + Z_2(\bar{A}_x + \bar{B}_u K_{SF}) \\ \Theta_{21} &= -Z_2^T + Z_1(\bar{A}_x + \bar{B}_u K_{SF}) \\ \Theta_{22} &= P - Z_2 - Z_2^T, \\ \Theta_{41} &= \bar{C}_{zx} + \bar{D}_{zu} K_{SF} \end{aligned}$$

and N is given by

$$N := \begin{bmatrix} 0 & * & * & * & * \\ 0 & 0 & * & * & * \\ \Phi_2 \bar{C}_{yx} - \Phi_1 K_{SF} & 0 & -\Phi_1 - \Phi_1^T & * & * \\ 0 & 0 & 0 & 0 & * \\ 0 & 0 & \bar{D}_{yw}^T \Phi_2^T & 0 & 0 \end{bmatrix} \tag{50}$$

with

$$\Phi_1 = \begin{bmatrix} Q & 0 \\ 0 & X_1 \end{bmatrix}, \quad \Phi_2 = \begin{bmatrix} H & 0 \\ 0 & X_2 \end{bmatrix}$$

Proof. Similar to the proof in [31], the expression in (46) can be rewritten as

$$U \Phi_1 V^T + V \Phi_1^T U^T + M \prec 0, \tag{51}$$

where V and U are defined as

$$V := \begin{bmatrix} \Phi_1^{-1}\Phi_2 \bar{C}_{yx} - K_{SF} & 0 & -I & 0 & \Phi_1^{-1}\Phi_2 \bar{D}_{yw} \end{bmatrix}^T, \tag{52}$$

$$U := \begin{bmatrix} 0 & 0 & I & 0 & 0 \end{bmatrix}^T. \tag{53}$$

Choosing the matrices,

$$N_V = \begin{bmatrix} I & 0 & 0 & 0 \\ 0 & I & 0 & 0 \\ \Phi_1^{-1}\Phi_2 \bar{D}_{yw} & 0 & 0 & \Phi_1^{-1}\Phi_2 \bar{C}_{yx} - K_{SF} \\ 0 & 0 & I & 0 \\ I & 0 & 0 & I \end{bmatrix} \tag{54}$$

$$N_U = \begin{bmatrix} I & 0 & 0 & 0 \\ 0 & I & 0 & 0 \\ 0 & 0 & 0 & 0 \\ 0 & 0 & I & 0 \\ 0 & 0 & 0 & I \end{bmatrix} \tag{55}$$

whose columns form the null spaces of V, and U, respectively. Then, according to the Projection lemma, the expression in (51) is equivalent to

$$\begin{bmatrix} A_{cl}^T Z_1^T + Z_1 A_{cl} - P & * & * & * \\ -Z_1^T + Z_2 A_{cl} & P - Z_2 - Z_2^T & * & * \\ C_{cl} & 0 & -I & * \\ B_{cl}^T Z_1^T & B_{cl}^T Z_2^T & D_{cl}^T & -\gamma^2 I \end{bmatrix} \prec 0 \tag{56}$$

which is a multiplication of M in (51) by N_V^T on the left and N_V on the right. Replacing K in (34)–(37), with $\Phi_1^{-1}\Phi_2$, guarantees the stability of the closed-loop system when using the static output feedback controller. Multiplying M in (51) by N_U^T on the left and N_U on the right gives the second condition in the Projection Lemma and ensures stability for the system when using the state feedback controller K_{SF}. The resulting expression is the same as in (56), but with K_{SF} replacing the static output feedback controllers for A_{cl}, B_{cl}, C_{cl}, and D_{cl}. Finally, multiplying (56) with β^T on the left and β on the right, with

$$\beta = \begin{bmatrix} I & 0 & 0 \\ A_{cl} & B_{cl} & 0 \\ 0 & 0 & I \\ 0 & I & 0 \end{bmatrix} \tag{57}$$

results in the bounded real lemma.

The optimization problem in (44)–(48) requires solving a bilinear matrix inequality (BMI), which is NP-hard and thus, difficult

to solve. However, by specifying a stable state feedback gain K_{SF}, it becomes a linear matrix inequality (LMI), and an iterative algorithm can be used to find a local optimum, following the procedure described in Algorithm 2. The controller parameters and measurement combination can be obtained from $K_i = X_1^{-1}X_2$ and $\hat{H} = Q^{-1}H$.

Algorithm 2:

Initialize: choose a stabilizing state feedback gain K_{SF}.

1: For fixed K_{SF}, solve the LMI:
$J_{k,1} = \min_{Z_1,Z_2,P,X_1,X_2,Q,H} \gamma^2$
s.t. (45), (46), (47), and (48)

2: Fix Z_1, Z_2, X_1, and Q at the values obtained in step 1 and solve the LMI:
$J_{k,2} = \min_{K_{SF},P,X_2,H} \gamma^2$
s.t. (45), (46), and (48).

3: If $J_{k,1} - J_{k,2} < \epsilon$ stop, else update K_{SF} and repeat step 1 to 3.

If Algorithm 2 is initialized with a stabilizing feedback gain K_{SF} such that step 1 gives a feasible solution for the first iteration, then it will generate a sequence of non-increasing solutions such that:

$$J_{k+1,1} \leq J_{k,2} \leq J_{k,1}, \quad \forall k$$

Remark 3. If an optimal measurement combination H_{opt} has been obtained *a priori* using e.g., (10) and (11), then Algorithm 2 can be modified by replacing the augmented measurement matrices $\bar{C}_{yx}$ and $\bar{D}_{yw}$ in (29) with

$$\bar{C}_{yx} = \begin{bmatrix} H_{opt}C_{yx} & 0 \\ 0 & I \end{bmatrix}, \quad \bar{D}_{yw} = \begin{bmatrix} H_{opt}D_{yw} \\ 0 \end{bmatrix}.$$

This results in the controller $K_i = X_1^{-1}X_2$ and a new measurement combination $\hat{H} = Q^{-1}HH_{opt}$ that gives the same steady-state loss, but should improve the dynamic behaviour of the closed-loop system.

4.3. Static output feedback and self-optimizing control

In the previous section, the problem of finding PI controllers and a measurement combination, $\hat{H}$ that minimizes the H_∞ norm of the closed-loop system was investigated, while in Section 3.2 the optimal trade-off between steady-state loss and the number of measurements used was considered. These two problems can easily be combined, resulting in the following optimization problem:

$$J_k = \min_{\substack{K_{SF},Z_1,Z_2,P \\ X_1,X_2,Q,H}} \gamma^2 + \alpha\frac{1}{2}\|HY\|_F^2 + \lambda\sum_{i,j} W_j\|H_{i,j}\|_1 \tag{58}$$

s.t. (11), (45), (46), (47), and (48)

The iterative procedure, described in Algorithm 3 can be used to find a local optimum, where the controller parameters and measurement combination can be obtained from $K_i = X_1^{-1}X_2$ and $\hat{H} = Q^{-1}H$ respectively.

Algorithm 3:

Initialize: choose a stabilizing state feedback gain K_{SF} and obtain H by solving (10) subject to (11) for all available measurements.

1: Compute $W^{(k)}$ using (18).

2: For the fixed K_{SF}, and $W^{(k)}$ solve the LMI:
$$J_{k,1} = \min_{\substack{Z_1,Z_2,P \\ X_1,X_2,Q,H}} \gamma^2 + \alpha\frac{1}{2}\|HY\|_F^2 + \lambda\sum_{i,j} W_j^{(k)}\|H_{i,j}\|_1$$
Subject to: (11), (45), (46), (47), and (48).

3: Update $W^{(k)}$ using (18) with the H obtained from step 2.

4: Fix Q, X_1, Z_1, and Z_2 at values obtained in step 2 and solve the LMI:
$$J_{k,2} = \min_{\substack{K_{SF},P,X_2,H}} \gamma^2 + \alpha\frac{1}{2}\|HY\|_F^2 + \lambda\sum_{i,j} W_j^{(k)}\|H_{i,j}\|_1$$
Subject to: (11), (45), (46), and (48).

5: If $\|H^{(k-1)} - H^{(k)}\|_2 < \epsilon_1$, and $J_{k,1} - J_{k,2} < \epsilon_2$ go to step 6, else update K_{SF} and repeat step 1 to 5.

6: Remove the measurements that correspond to the zero columns in H.

The convergence of Algorithm 3 follows the convergence properties of Algorithms 1 and 2. When $\lambda = 0$ then the convergence is monotonically decreasing:

$$J_{k+1,1} \leq J_{k,2} \leq J_{k,1}, \quad \forall k$$

If the re-weighted l_1-norm is incorporated, then the convergence is unknown. However, numerical experiments (e.g., [23,30]) indicates that it tends to converge to a local minimum.

5. Simulations

In this section, the effectiveness of the proposed algorithms is validated by application to two different distillation column models. The optimization problems were formulated by the YALMIP toolbox [39] and solved using the solver MOSEK [40].

5.1. Binary distillation column

In the first example, the proposed algorithms are applied to the "column A" distillation column model [41], where a binary mixture is separated that has a relative volatility of 1.5. The distillation column has 41 stages, which includes the reboiler and the condenser. The stages are counted from the bottom with the reboiler as stage 1 and with the feed at stage 21. For the distillation column, the feed is assumed to be given. Thus, it has four degrees of freedom; bottoms flow rate (B), distillate flow rate (D), reflux flow rate (L_R) and vapor boilup (V_B). The distillate boilup and bottom flow rate are used to stabilize the two liquid levels in the condenser and the reboiler. This results in the LV configuration shown in Fig. 3 where the two remaining degrees of freedom are:

$$u = \begin{bmatrix} L_R & V_B \end{bmatrix}^T. \tag{59}$$

The objective is to get a top product with 99% light component (1% heavy) and a bottom product with 1% light component, i.e., the cost function is

$$J = \left(\frac{x_H^{top} - x_H^{top,s}}{x_H^{top,s}}\right)^2 + \left(\frac{x_L^{btm} - x_L^{btm,s}}{x_L^{btm,s}}\right)^2, \tag{60}$$

where the specifications for the top and bottom products are denoted with the superscript, s.

As composition often is difficult to measure, they will be controlled indirectly using the temperatures inside the column as in [25]. It is assumed that the temperatures $T_i(^\circ C)$ on each stage i can be calculated using the linear function [41],

$$T_i = 0x_{L,i} + 10x_{H,i} \tag{61}$$

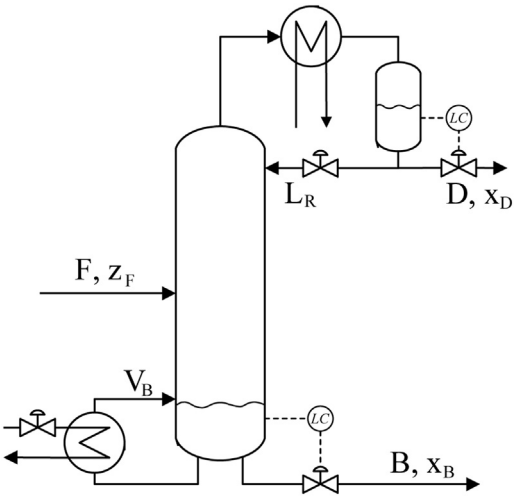

Fig. 3. A typical distillation column with LV configurations.

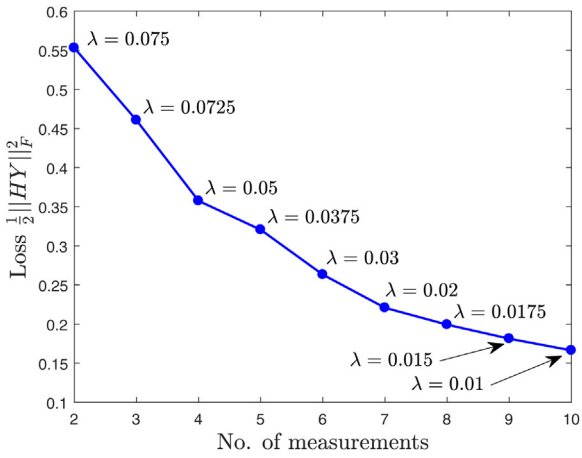

Fig. 4. Steady-state loss vs no. of measurements for the binary distillation column.

Table 1
Controlled variables for steady-state loss, where c_{opt} [28] is compared to c_{alg}, which has been obtained using Algorithm 1.

No. meas.	Controlled variables	Loss $\frac{1}{2}\|HY\|_F^2$
2	$c_{opt} = \begin{bmatrix} T_{12} \\ T_{30} \end{bmatrix}$	0.548
	$c_{alg} = \begin{bmatrix} T_{12} \\ T_{29} \end{bmatrix}$	0.553
3	$c_{opt} = \begin{bmatrix} T_{12} + 0.0446T_{31} \\ T_{30} + 1.0216T_{31} \end{bmatrix}$	0.443
	$c_{alg} = \begin{bmatrix} T_{12} + 1.3030T_{13} \\ T_{29} - 0.0705T_{13} \end{bmatrix}$	0.463
4	$c_{opt} = \begin{bmatrix} 1.0316T_{11} + T_{12} + 0.0993T_{31} \\ 0.0891T_{11} + T_{30} + 1.0263T_{31} \end{bmatrix}$	0.344
	$c_{alg} = \begin{bmatrix} 1.0811T_{12} + T_{13} + 0.2075T_{30} \\ 0.1205T_{12} + T_{29} + 1.0859T_{30} \end{bmatrix}$	0.358

with an accuracy of $\pm 0.5\,^{\circ}C$.

The main disturbances considered are changes in feed flow rate (F), feed composition (z_F) and feed liquid fraction (q_F), where F and z_F can vary between 1 ± 0.2, and 0.5 ± 0.1 respectively. The nominal value for q_F is 1.0 with a lower bound of 0.9.

5.1.1. Measurement selection for steady-state loss

Finding the optimal subset of measurements that minimizes the steady-state loss for the binary distillation column example has previously been studied in [29,28]. The problem was solved in [29] with a branch and bound method, while in [28] a MIQP formulation was used. The optimal controlled variables and their respective steady-state loss when using 2, 3, and 4 measurements obtained from [28] can be seen in Table 1.

The optimal controlled variables are compared to controlled variables computed using Algorithm 1. The trade-off between the steady-state loss and the number of measurement used can be seen in Fig. 4 when using different values for λ (obtained using trial and error). The measurement combination H for sets of 2, 3, and 4 measurements, can be seen in Table 1.

Algorithm 1 promotes sparsity, using the weighted l_1-norm as a convex relaxation for the cardinality of the H matrix. As a consequence, it cannot guarantee that it converges to the optimal measurement subset and therefore, it gives subsets with a slightly larger steady-state loss compared to the ones obtained in [28].

5.1.2. Dynamic and steady-state performance

For the optimal control variable when using 3 measurements (in Table 1), the author of [42] implemented two PI controllers, that were tuned using the SIMC method [43] and resulted in $c_{A,3}$ shown in Table 2. However, by using Algorithm 2 as described in Remark 3, it should be possible to find a different measurement combination ($c_{B,3}$) together with PI controllers that further improves the transient response, without affecting the steady-state loss. Similarly, a controlled variable when using the 4 optimal measurements given in Table 1 is also obtained, using the same procedure, resulting in $c_{A,4}$. For comparison Algorithm 3 is used to find a $c_{B,4}$, which should give an improvement in the dynamic behaviour at the expense of the steady-state loss. Finally, the controlled variables $c_{A,7}$, and $c_{B,7}$ are computed when using 7 measurements. The controlled variable $c_{A,7}$ puts more emphasis on the steady-state loss (large α), while $c_{B,7}$ priorities the dynamic performance of the resulting closed-loop system (small α). All the controlled variables $c_{A,n}$, and $c_{B,n}$ (n defines the number of measurements) can be seen in Table 2, together, with their respective H_∞-norm and steady-state loss.

Out of the three disturbances F, z_F, and q_F, changes in feed flow F have no steady-state effect on the cost. Therefore, the dynamic performance for changes in F is only considered, as it makes it easier to compare the transient responses. The simulation for a step change in F can be seen in Fig. 5, and shows a significant improvement in the response for $c_{B,3}$ obtained using Algorithm 2 compared to $c_{A,3}$ that was proposed in [42]. As expected, a better response is also achieved for $c_{B,4}$ compared to $c_{A,4}$, when a trade-off between minimizing the H_∞-norm and steady-state loss is computed using Algorithm 3. It is interesting to note that using 7 measurements ($c_{A,7}$ and $c_{B,7}$), gives the best and nearly the worst dynamic response depending on whether the focus lies on minimizing the H_∞-norm of the closed-loop system or the steady-state performance. This would suggest that the dynamic considerations when selecting measurement combinations become more crucial, the more measurements are used. Furthermore, $c_{B,7}$ also has the second lowest steady-state loss and thus, it can be seen that a small sacrifice in steady-state loss might give a significant improvement in the control performance.

5.2. Kaibel distillation column

A Kaibel distillation column [44] is a thermally coupled distillation column that can separate four products using a single condenser and a single reboiler (see Fig. 6). To achieve the same four product streams from a single feed stream when using conventional binary columns, it would require a setup consisting of three different binary columns.

A Kaibel distillation column is an extension to the Petlyuk distillation column [45] and has together with other diving wall columns, to a great extent been studied in the literature [46]. In comparison

Table 2
Controlled variables, PI parameters ($K_p = I$), and their dynamic and steady-state performance for the binary distillation column.

Controlled variables	K_i	$\|T_{w,z}\|_\infty$	$\frac{1}{2}\|HY\|_F^2$
$c_{A,3} = \begin{bmatrix} -0.022T_{12} + 0.383T_{30} + 0.390T_{31} \\ -0.906T_{12} + 0.149T_{30} + 0.111T_{31} \end{bmatrix}$	0.125 0.125	0.343	0.443
$c_{B,3} = \begin{bmatrix} -2.289T_{12} + 0.451T_{30} + 0.358T_{31} \\ -3.715T_{12} - 0.818T_{30} - 1.001T_{31} \end{bmatrix}$	0.175 0.145	0.074	0.443
$c_{A,4} = \begin{bmatrix} -0.970T_{11} - 0.923T_{12} - 0.200T_{30} - 0.297T_{31} \\ -1.093T_{11} - 1.040T_{12} - 0.227T_{30} - 0.336T_{31} \end{bmatrix}$	0.164 0.173	0.144	0.344
$c_{B,4} = \begin{bmatrix} -0.479T_{11} - 0.479T_{12} + 1.110T_{32} + 0.852T_{33} \\ -0.782T_{11} - 0.801T_{12} - 1.265T_{32} - 1.147T_{33} \end{bmatrix}$	0.601 0.736	0.070	0.383
$c_{A,7} = \begin{bmatrix} -0.118T_{11} - 0.128T_{12} - 0.123T_{13} - 0.015T_{21} + 0.125T_{28} + 0.139T_{29} + 0.126T_{30} \\ -0.204T_{11} - 0.220T_{12} - 0.209T_{13} + 0.090T_{21} + 0.062T_{28} + 0.054T_{29} + 0.030T_{30} \end{bmatrix}$	0.170 0.206	0.341	0.222
$c_{B,7} = \begin{bmatrix} -0.272T_{11} - 0.276T_{12} - 0.267T_{13} + 0.251T_{25} + 0.645T_{32} + 0.530T_{33} + 0.416T_{34} \\ -0.536T_{11} - 0.528T_{12} - 0.505T_{13} + 0.244T_{25} - 1.055T_{32} - 0.971T_{33} - 0.784T_{34} \end{bmatrix}$	0.624 0.731	0.066	0.271

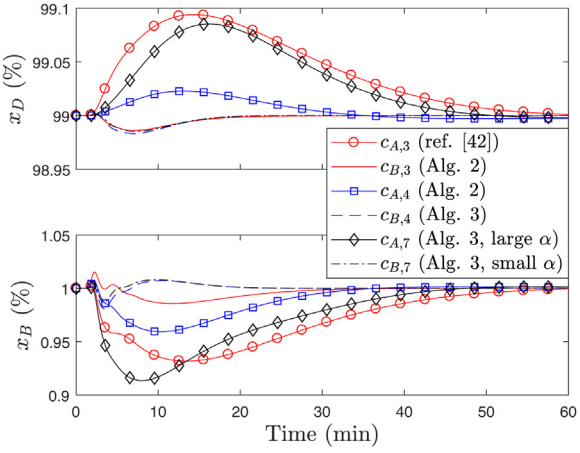

Fig. 5. Distillate and bottom compositions changes in the binary distillation column for a step disturbance of −10% in F.

to the traditional configurations, the Kaibel column has the potential to give up to 40% reduction in energy consumption, as well as significantly reducing the capital investment cost and the physical space required in the process plant. However, the energy savings are only achieved if the distillation column operates close to its optimal value, which remains a challenge as it is a highly interactive multivariable system that is difficult to control.

The Kaibel column is dived into seven sections, and each section consists of several stages. For the simulated model, there are a total of 64 stages as shown in Fig. 6, where the stages are numbered with the prefractionator section first. The ternary feed is located between stage 12 and 13 and consists of three components with the mole fractions z_D, z_{S_1}, and z_{S_2}. Four product streams are drawn of, where the light component z_D dominates the distillate stream (D), component z_{S_1} and z_{S_2} dominate in the side-streams (S_1, and S_2) and the remaining heavy components z_B dominates the bottom stream (B). For a more detailed description of the process model and its nominal values, the reader is referred to [47].

The distillate boilup (D) and bottom flow rate (B) are used to stabilize the levels in the condenser and the reboiler, respectively. Furthermore, vapor boilup V_B and the vapor split R_V will be kept constant as it has been shown to be difficult to control in practice. Instead, they will be treated as disturbances. Therefore, the remaining degrees of freedom u and disturbances d are:

$$u = \begin{bmatrix} R_L & L_R & S_1 & S_2 \end{bmatrix}^T \tag{62}$$

$$d = \begin{bmatrix} V_B & R_V & F & z_D & z_{S_1} & z_{S_2} & q_F \end{bmatrix}^T. \tag{63}$$

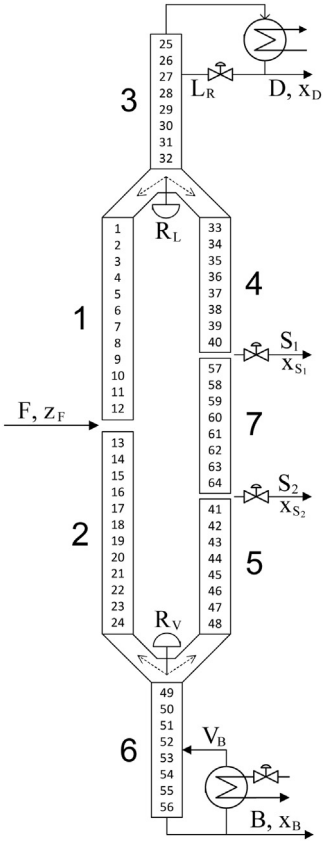

Fig. 6. Kaibel distillation column.

For the Kaibel column, the objective is to optimize the product distribution for given feed rate F and boilup rate V_B. Assuming equal value of the products and that only the main components in each product stream are of value, then the objective is equivalent to minimizing the sum of the impurity flows. The cost function J can then be written as [48]:

$$J = D(1 - x_D) + S_1(1 - x_{S_1}) + S_2(1 - x_{S_2}) + B(1 - x_B). \tag{64}$$

5.2.1. Control structure design

The control structure design for the Kaibel column model has previously been studied in [47–49]. Most of the work has mainly been focused on the steady-state operation of the column; however, different control structures was presented in [49].

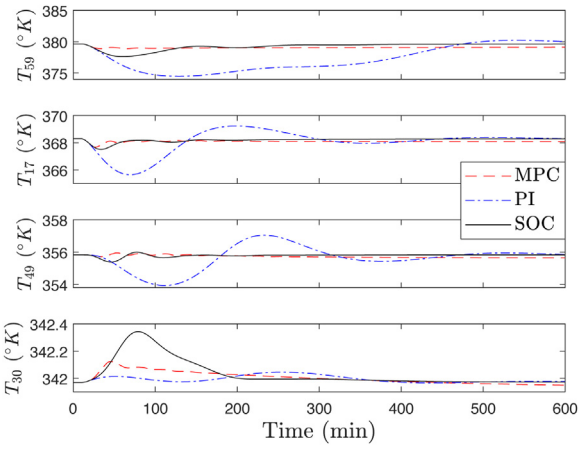

Fig. 7. Temperature changes in the Kaibel column for a step disturbance of +10% in F.

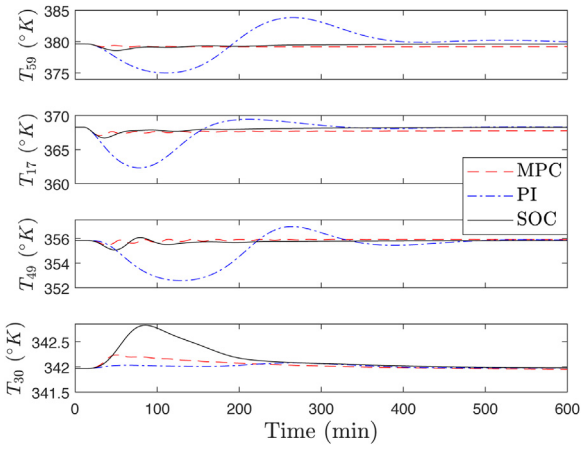

Fig. 8. Temperature changes in the Kaibel column for a step disturbance of +20% in z_{S_1}.

Using the temperatures at stages 17, 30, 49, and 59 as the available measurements,

$$y = \begin{bmatrix} T_{17} & T_{30} & T_{49} & T_{59} \end{bmatrix}^T, \tag{65}$$

decentralized PI control was designed for the Kaibel column in [49], where the PI controllers were tuned using the SIMC tuning rules [43]. Controlling the temperatures in (65) had been shown to possess good self-optimizing control properties based on the singular value method [6]. However, due to the high level of process interactions, it was difficult to achieve good control performance using only decentralized PI controllers. Therefore, the authors of [49] proposed using an MPC to better counteract the interactions and obtain less total impurity flow. These two control structures will be used as comparison in the dynamic simulation and are denoted MPC and PI.

The decentralized PI controllers in [49] are controlling each of the measurements in (65) individually. However, since the number of control inputs is equal to the number of measurements ($n_u = n_y$), it is possible to choose a controlled variable $c = \hat{H}y$ with any measurement combination $\hat{H}$ (assuming $\hat{H}$ is invertible) and still get the same the steady state loss. This can be demonstrated by selecting $Q = \hat{H}$, which according to (12), gives $H = Q^{-1}\hat{H} = I$. Therefore, using Algorithm 2, a measurement combination

$$\hat{H} = \begin{bmatrix} 0.0209 & -0.0013 & -0.0002 & -0.0096 \\ 0.0171 & 0.0292 & -0.0009 & 0.0132 \\ -0.0237 & 0.0274 & 0.0019 & -0.0247 \\ 0.0230 & 0.0052 & -0.0270 & 0.0224 \end{bmatrix}, \tag{66}$$

and PI parameters

$$K_p = I, \quad K_i = \begin{bmatrix} 0.0074 & 0 & 0 & 0 \\ 0 & 0.0149 & 0 & 0 \\ 0 & 0 & 0.0073 & 0 \\ 0 & 0 & 0 & 0.0088 \end{bmatrix} \tag{67}$$

can be obtained for the same measurements given in (65). The proposed control structure is denoted SOC and should give a better dynamic performance compared to the decentralized PI controllers in [49].

5.2.2. Dynamic simulation

Dynamic simulations were performed on the non-linear model of the Kailbel distillation column. In Figs. 7–9, changes in the controlled temperatures T_{17}, T_{30}, T_{49}, and T_{59} are simulated for step changes in the disturbances F, z_{S_1}, and R_V. Compared to the decentralized PI controllers, there is a significant improvement in the transient response when using the proposed measurement combination *SOC*. Furthermore, in the resulting impurity flows shown in Figs. 10–12, the proposed control structure seems to be on par with the MPC.

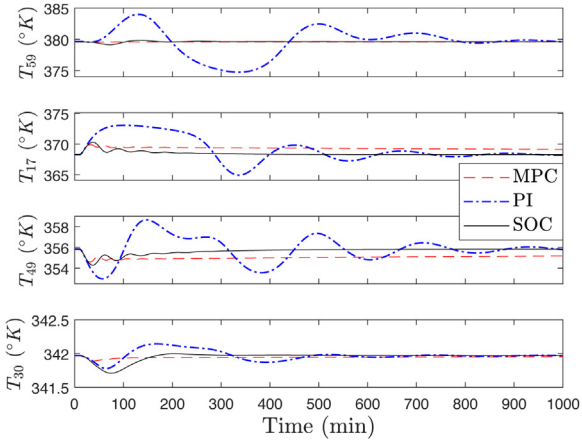

Fig. 9. Temperature changes in the Kaibel column for a step disturbance of +10% in R_V.

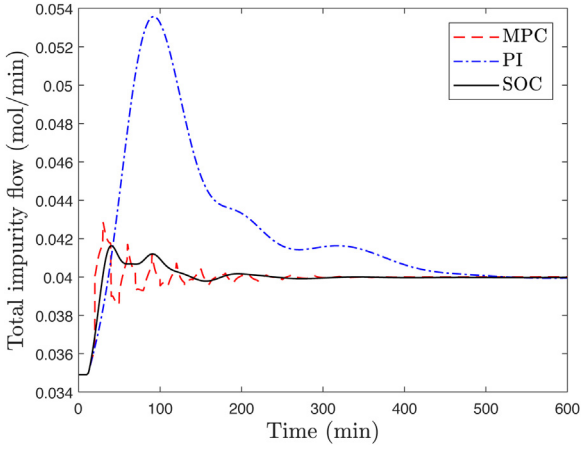

Fig. 10. Impurity flow (64) for a step disturbance of +10% in F.

These results are particularly interesting, as it would suggest that by properly selecting controlled variables (measurement combinations) together with well-tuned PI controllers, it might be

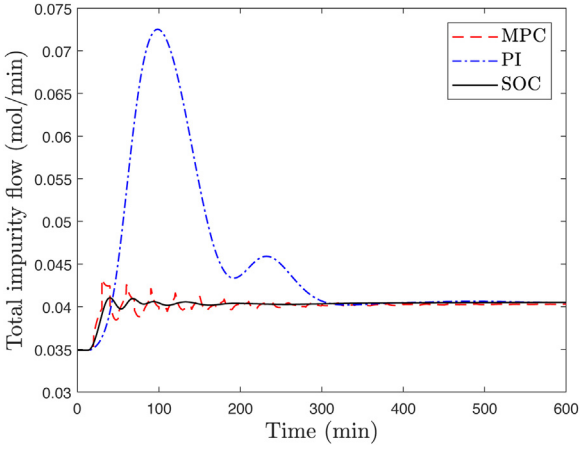

Fig. 11. Impurity flow (64) for a step disturbance of +20% in z_{s_1}.

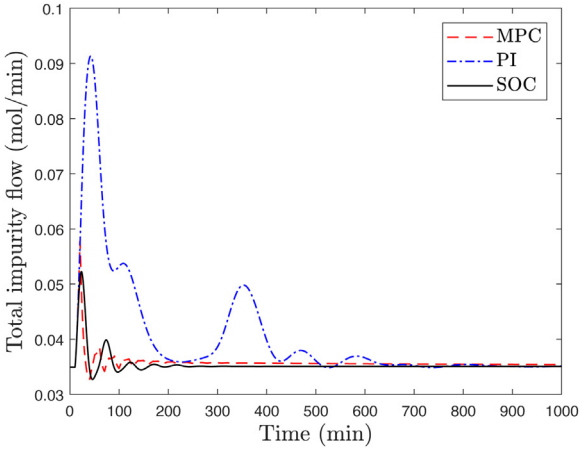

Fig. 12. Impurity flow (64) for a step disturbance of +10% in R_V.

possible to compete with a control structure consisting of an MPC combined with real-time optimization.

6. Conclusion

In this work, the transient behaviour when selecting the self-optimizing control variable has been considered. The main objective has been to develop an algorithm that computes the measurement combination together with PI controllers and gives the optimal trade-off between dynamic and steady-state performance. A penalty function can also be included that penalizes the number of measurement used and attempts to find a subset for the desired trade-off. The proposed algorithms can't guarantee a globally optimal solution as they converge to a local minimum. The focus of this work is on simultaneous control structure and controller design, and not on the solution of BMIs. Therefore, the use of global optimization solvers for the resulting BMI problems [50] have not been investigated. However, two non-trivial examples demonstrate that good results are found both with respect to the (near) optimality of the steady-state solution, and the control performance of the resulting closed-loop system.

References

[1] S. Skogestad, Control structure design for complete chemical plants, Comput. Chem. Eng. 28 (1–2) (2004) 219–234.
[2] J.J. Downs, S. Skogestad, An industrial and academic perspective on plantwide controls, Annu. Rev. Control 35 (1) (2011) 99–110.
[3] D. Müller, B. Dercks, E. Nabati, M. Blazek, T. Eifert, J. Schallenberg, U. Piechottka, K. Dadhe, Real-time optimization in the chemical processing industry, Chem. Ing. Tech. 89 (11) (2017) 1464–1470.
[4] M. Ellis, H. Durand, P.D. Christofides, A tutorial review of economic model predictive control methods, J. Process Control 24 (8) (2014) 1156–1178.
[5] S. Skogestad, Plantwide control: the search for the self-optimizing control structure, J. Process Control 10 (5) (2000) 487–507.
[6] I.J. Halvorsen, S. Skogestad, J.C. Morud, V. Alstad, Optimal selection of controlled variables, Ind. Eng. Chem. Res. 42 (14) (2003) 3273–3284.
[7] V. Alstad, S. Skogestad, Null space method for selecting optimal measurement combinations as controlled variables, Ind. Eng. Chem. Res. 46 (3) (2007) 846–853.
[8] J. Jäschke, Y. Cao, V. Kariwala, Self-optimizing control – a survey, Annu. Rev. Control 43 (2017) 199–223.
[9] K.J. Åstrom, T. Hägglund, The future of PID control, Control Eng. Pract. 9 (11) (2001) 1163–1175.
[10] A. Jayachitra, R. Vinodha, Genetic algorithm based PID controller tuning approach for continuous stirred tank reactor, Adv. Artif. Intell. (2014) 1–9.
[11] Z.-L. Gaing, A particle swarm optimization approach for optimum design of PID controller in AVR system, IEEE Trans. Energy Convers. 19 (2) (2004) 384–391.
[12] A. Karimi, M. Kunze, R. Longchamp, Robust controller design by linear programming with application to a double-axis positioning system, Control Eng. Pract. 15 (2) (2007) 197–208.
[13] M.S. Govatsmark, S. Skogestad, Selection of controlled variables and robust setpoints, Ind. Eng. Chem. Res. 44 (7) (2005) 2207–2217.
[14] E.B. Aske, S. Skogestad, S. Strand, Throughput maximization by improved bottleneck control, 8th International IFAC Symposium on Dynamics and Control of Process Systems 40 (5) (2007) 63–68.
[15] V.L. Syrmos, C.T. Abdallah, P. Dorato, K. Grigoriadis, Static output feedback – a survey, Automatica 33 (2) (1997) 125–137.
[16] M.S. Sadabadi, D. Peaucelle, From static output feedback to structured robust static output feedback: a survey, Annu. Rev. Control 42 (2016) 11–26.
[17] D. Peaucelle, D. Arzelier, An efficient numerical solution for H_2 static output feedback synthesis, European Control Conference (ECC) (2001) 3800–3805.
[18] Y. Ebihara, D. Peaucelle, D. Arzelier, S-variable approach to LMI-based robust control, in: Springer Series: Communications and Control Engineering, 2015.
[19] J.R.A. Klemets, M. Hovd, An iterative LMI approach to controller design and measurement selection in self-optimizing control, 11th Asian Control Conference (ASCC) (2017) 2849–2854.
[20] J.R.A. Klemets, M. Hovd, Controller design and sparse measurement selection in self-optimizing control, 10th IFAC Symposium on Advanced Control of Chemical Processes (ADCHEM) (2018) 458–463.
[21] E.J. Candes, M.B. Wakin, S.P. Boyd, Enhancing sparsity by reweighted l_1 minimization, J. Fourier Anal. Appl. 14 (5–6) (2008) 877–905.
[22] N.K. Dhingra, M.R. Jovanović, Z.-Q. Luo, An ADMM algorithm for optimal sensor and actuator selection, 53rd IEEE Conference on Decision and Control (2014) 4039–4044.
[23] M. Fardad, F. Lin, M.R. Jovanović, Sparsity-promoting optimal control for a class of distributed systems, American Control Conference (ACC) (2011) 2050–2055.
[24] F. Dörfler, M.R. Jovanović, M. Chertkov, F. Bullo, Sparsity-promoting optimal wide-area control of power networks, IEEE Trans. Power Syst. 29 (5) (2014) 2281–2291.
[25] E.S. Hori, S. Skogestad, V. Alstad, Perfect steady-state indirect control, Ind. Eng. Chem. Res. 44 (4) (2005) 863–867.
[26] V. Kariwala, Y. Cao, S. Janardhanan, Local self-optimizing control with average loss minimization, Ind. Eng. Chem. Res. 47 (4) (2008) 1150–1158.
[27] V. Alstad, S. Skogestad, E.S. Hori, Optimal measurement combinations as controlled variables, J. Process Control 19 (1) (2009) 138–148.
[28] R. Yelchuru, S. Skogestad, Convex formulations for optimal selection of controlled variables and measurements using mixed integer quadratic programming, J. Process Control 12 (6) (2012) 995–1007.
[29] V. Kariwala, Y. Cao, Bidirectional branch and bound for controlled variable selection. part II: Exact local method for self-optimizing control, Comput. Chem. Eng. 33 (8) (2009) 1402–1414.
[30] A. Argha, S.W. Su, A. Savkin, B. Celler, A framework for optimal actuator/sensor selection in a control system, Int. J. Control (2017).
[31] C.F. Morais, M.F. Braga, R.C.L.F. Oliveira, P.L.D. Peres, H_∞ static output feedback control of discrete-time Markov jump linear systems with uncertain transition probability matrix, American Control Conference (ACC) (2014) 489–494.
[32] C.M. Agulhari, R.C.L.F. Oliveira, P.L.D. Peres, Robust H_∞ static output-feedback design for time-invariant discrete-time polytopic systems from parameter-dependent state-feedback gains, American Control Conference (ACC) (2010) 4677–4682.
[33] H.R. Moreira, R.C.L.F. Oliveira, P.L.D. Peres, Robust H_2 static output feedback design starting from a parameter-dependent state feedback controller for time-invariant discrete-time polytopic system, Opt. Control Appl. Methods 32 (1) (2011) 1–13.
[34] D. Rosinová, A. Kozáková, Robust decentralized PID controller design, Introduction to PID Controllers – Theory, Tuning and Application to Frontier Areas (2012) 133–168.
[35] J.S. Lim, Y.I. Lee, Design of discrete-time multivariable PID controllers via LMI approach, International Conference on Control, Automation and Systems (2008) 1867–1871.

[36] P. Gahinet, P. Apkarian, A linear matrix inequality approach to H_∞ control, Int. J. Robust Nonlinear Control 4 (4) (1994).
[37] S. Skogestad, I. Postlethwaite, Multivariable Feedback Control: Analysis and Design, Wiley, 2005.
[38] G. Pipeleers, B. Demeulenaere, J. Swevers, L. Vandenberghe, Extended LMI characterizations for stability and performance of linear systems, Syst. Control Lett. 58 (7) (2009) 510–518.
[39] J. Löfberg, YALMIP: a toolbox for modeling and optimization in MATLAB, in: Proceedings of the CACSD Conference, Taipei, Taiwan, 2004, pp. 284–289.
[40] M. Aps, MOSEK, 2018 https://mosek.com/.
[41] S. Skogestad, Dynamics and control of distillation columns: a tutorial introduction, Chem. Eng. Res. Des. 75 (6) (1997) 539–562.
[42] R. Yelchuru, Quantitative Methods for Controlled Variables Selection (Ph.D. thesis), Norwegian University of Science and Technology, 2012.
[43] S. Skogestad, Simple analytic rules for model reduction and PID controller tuning, J. Process Control 13 (4) (2003) 291–309.
[44] G. Kaibel, Distillation columns with vertical partitions, Chem. Eng. Technol. 10 (1) (1987) 92–98.
[45] F. Petlyuk, V. Platonov, D. Slavinskii, Thermodynamically optimal method for separating multicomponent mixtures, Int. Chem. Eng 5 (3) (1965) 555–561.
[46] R.C. van Diggelen, A.A. Kiss, A.W. Heemink, Comparison of control strategies for dividing-wall columns, Ind. Eng. Chem. Res. 49 (1) (2010) 288–307.
[47] M. Kvernland, Model Predictive Control of a Kaibel Distillation Column (Master's thesis), Norwegian University of Science and Technology, 2009.
[48] J. Strandberg, Optimal Operation of Dividing Wall Columns (Ph.D. thesis), Norwegian University of Science and Technology, 2011.
[49] M. Kvernland, I. Halvorsen, S. Skogestad, Model predictive control of a Kaibel distillation column, 9th IFAC Symposium on Dynamics and Control of Process Systems 43 (5) (2010) 553–558.
[50] C.A. Floudas, Deterministic Global Optimization: Theory, Methods and Applications, Kluwer Academic Publishers, Dordrecht, 2000.